Amygdala in Action: Functional Connectivity during Approach and Avoidance Behaviors

Joana Leitão[1], Maya Burckhardt[2], and Patrik Vuilleumier[1]

Abstract

■ Motivation is an important feature of emotion. By driving approach to positive events and promoting avoidance of negative stimuli, motivation drives adaptive actions and goal pursuit. The amygdala has been associated with a variety of affective processes, particularly the appraisal of stimulus valence that is assumed to play a crucial role in the generation of approach and avoidance behaviors. Here, we measured amygdala functional connectivity patterns while participants played a video game manipulating goal conduciveness through the presence of good, neutral, or bad monsters. As expected, good versus bad monsters elicited opposing motivated behaviors, whereby good monsters induced more approach and bad monsters triggered more avoidance. These opposing directional behaviors were paralleled by increased connectivity between the amygdala and medial brain areas, such as the OFC and posterior cingulate, for good relative to bad, and between amygdala and caudate for bad relative to good monsters. Moreover, in both conditions, individual connectivity strength between the amygdala and medial prefrontal regions was positively correlated with brain scores from a latent component representing efficient goal pursuit, which was identified by a partial least squares analysis determining the multivariate association between amygdala connectivity and behavioral motivation indices during gameplay. At the brain level, this latent component highlighted a widespread pattern of amygdala connectivity, including a dorsal frontoparietal network and motor areas. These results suggest that amygdala-medial prefrontal interactions captured the overall subjective relevance of ongoing events, which could consecutively drive the engagement of attentional, executive, and motor circuits necessary for implementing successful goal-pursuit, irrespective of approach or avoidance directions. ■

INTRODUCTION

The functional and neuroanatomical organization of affective processes remains unresolved despite important progress during the past 2 decades in mapping widespread brain networks involved in emotion and cognition. Different theoretical approaches in psychology have emphasized different behavioral aspects of emotion, such as appraisal, expression, or action tendencies (Moors, 2014; Scherer, 2001; Frijda, 1987), whereas neuroscience research has generally focused on investigating brain areas engaged by particular categories of emotions such fear, anger, disgust, or pleasure (Vytal & Hamann, 2010), or different modalities of emotional signals such as faces, voices, or smells (Meaux & Vuilleumier, 2015). However, there is a growing consensus that emotions comprise multiple components, possibly combined in interactive ways during elicitation episodes (Leitão, Meuleman, Van De Ville, & Vuilleumier, 2020; Barrett, 2017). Among influential models, some posit that all emotions are governed by two separate functional systems representing valence (i.e., relative degrees of pleasantness or unpleasantness) and arousal (i.e., relative degrees of activation or inhibition; Russell, 2003), integrated with higher-level cognitive categorization processes (Barrett, 2017), whereas others consider emotions as emerging from contextual appraisals that drive parallel changes in motivation, expression, physiology, and subjective feeling (Scherer, 2009).

Across these different theoretical views, it is generally thought that a central feature of emotions is their capacity to influence goal-directed behaviors, promoting approach or avoidance based on the valence (e.g., dimensional models) or the motivational relevance (e.g., appraisal models) of situational cues. However, to ensure adaptive responses, motivated behavior must integrate environmental stimuli and internal needs in a flexible manner in order to select appropriate actions and thus attain short- or long-term goals. Approaching or avoiding a particular stimulus or situation might be beneficial in some contexts, but not in others. Motivational systems should therefore not only encode the intrinsic value of stimuli and their behavioral relevance but also deploy context-dependent mechanisms promoting advantageous actions and suppressing unfavorable options depending on current goals. Yet, the neural systems underlying this modulation of motivated actions in response to affectively relevant events are still largely unknown.

Based on dimensional models of emotion directly linking approach versus avoidance tendencies to the pleasant/appetitive versus unpleasant/aversive value of sensory

This article is part of a Special Focus entitled "Contemporary Approaches to Emotion Representation".

[1]University of Geneva, Switzerland, [2]University of Fribourg, Switzerland

cues, respectively, several studies investigated simple motor actions directed toward or away from a stimulus (e.g., pictures, words, facial expressions) associated with positive or negative valence. For example, in one of the earliest studies (Solarz, 1960), participants saw pleasant and unpleasant words on cards presented on a movable stage that could be either pulled toward or pushed away from them, and participants had to adjust their responses according to feedback on their choice accuracy. Results showed that approach movements were faster during the presentation of positive stimuli, whereas avoidance movements were faster to negative stimuli. Similar findings have been reported in various paradigms with different response modalities (i.e., directional: joystick, arm flexion/extension—or nondirectional: button press) and different response mappings (i.e., using push–approach and pull–avoid associations or vice versa; Laham, Kashima, Dix, & Wheeler, 2015; Phaf, Mohr, Rotteveel, & Wicherts, 2014). This so-called affective compatibility effect is characterized by a facilitation of responses when the behavioral goal is congruent with stimulus valence, whereas responses are slower in incongruent conditions presumably because of control mechanisms acting to overwrite automatic emotional action tendencies. Neuroimaging studies also explored the neural underpinnings of these (implicit) approach and avoidance actions in relation to valence (Ascheid, Wessa, & Linke, 2019; Cunningham, Arbuckle, Jahn, Mowrer, & Abduljalil, 2011; Berkman & Lieberman, 2010), or stimulus–goal incongruence (Bramson et al., 2020; Kaldewaij, Koch, Volman, Toni, & Roelofs, 2017; Roelofs, Minelli, Mars, van Peer, & Toni, 2009). These studies found activations in several limbic areas such as the OFC and amygdala, as well as the anterior and lateral pFC, ACC, and basal ganglia. These areas might constitute a motivation-driving network responsible for instantiating approach and avoidance behaviors (Spielberg et al., 2012). Other neuroimaging studies used adaptive free-choice tasks, in which actions were linked to positive or negative consequences for the participant (Schlund, Magee, & Hudgins, 2011; Schlund & Cataldo, 2010; Kim, Shimojo, & O'Doherty, 2006), and reported that approach and avoidance engage similar brain structures including the amygdala, medial and ventral prefrontal areas, as well as distributed fronto-parieto-striatal areas. This overlap might reflect the fact that successful approach and avoidance behaviors equally require the recruitment of attentional processes and action preparation (Lang & Bradley, 2013), putatively orchestrated by medial prefrontal areas and the amygdala. However, it has also been proposed that such overlap could partly be explained by the fact that avoidance of an aversive outcome, if successful, can itself be rewarding and hence recruit similar neural circuits as approaching a positive event (Schlund et al., 2011; Kim et al., 2006). In other words, these regions might encode affective properties of goal attainment irrespective of motivational direction.

Here, we investigated approach and avoidance using an interactive video game paradigm in which participants could freely adjust their actions in response to goal-conducive (positive) or goal-obstructive (negative) manipulations that were directly self-relevant in terms of the game goals. According to most appraisal theories of emotions, goals play an important role in triggering emotional responses (Moors, Boddez, & De Houwer, 2017) and constitute "cognitive representations of a future object that an individual is committed to approach or avoid" (Elliot & Fryer, 2008). Unlike previous motor tasks using dichotomous predefined categories of stimuli or actions, our paradigm enabled us to assess different facets of motivated behavior through multiple indices of self-initiated behavior, measured simultaneously during proactive game performance. To determine changes in brain activity associated with distinct motivational states, we acquired fMRI in participants while they played the game and examined variations in functional connectivity of the amygdala with the rest of the brain across different game conditions and different behavioral patterns.

The amygdala is implicated in a wide range of affective processes (Phelps & LeDoux, 2005) and thought to play a crucial role in the control of motivated behaviors (Janak & Tye, 2015), as it appears ideally placed not only for encoding the value of environmental stimuli but also for mobilizing resources and influencing motor actions according to ongoing goals and internal needs (Freese & Amaral, 2009; Amaral & Price, 1984). Although classically associated with fear and defense-related responses (LeDoux, 2012), the amygdala also responds to positive valence (Baxter & Murray, 2002) and may have a more general valuation function (Morrison & Salzman, 2010). Accordingly, it has been argued that the amygdala could act as a relevance detector (Sander, Grafman, & Zalla, 2003), in line with appraisal theories of emotions (Moors, 2014; Scherer, 2001) whereby processing the significance of external events as a function of current goals or needs is the primary step for eliciting an emotional response. As such, the amygdala would allow for the ongoing appraisal of environmental stimuli, incorporating not only their intrinsic value but also their state-dependent representation in terms of immediate behavioral implications (Cunningham & Brosch, 2012; Belova, Paton, & Salzman, 2008). This view is supported by lesion studies in primates (Izquierdo & Murray, 2007; Murray & Izquierdo, 2007) showing that an intact amygdala is necessary not only to learn and react to the affective value of stimuli but also to attenuate behavioral responses to devaluated stimuli (e.g., food to which the animal has previously been exposed until satiation). Likewise, in humans, food-related visual stimuli elicit greater activation in the amygdala when participants are in a hungry relative to a satiated state (LaBar et al., 2001). Hence, amygdala activity appears to be centrally involved in both appetitive/approach and aversive/avoidance processing.

Therefore, we hypothesized that amygdala responses to relevant events might be differentially coupled with other brain areas depending on current goals and specific

directions of motivated behaviors. The amygdala could indeed exert potent effects on behavior and motivation through its widespread projections to brain networks associated with attention, action, and autonomic functions, engaging the necessary sensorimotor and executive resources once an emotional stimulus is deemed relevant and requires to be acted upon (Phelps & LeDoux, 2005). Moreover, the amygdala also acts to modulate attention orienting to relevant features of emotionally significant stimuli (Kim et al., 2017; Vuilleumier & Pourtois, 2007; Adolphs et al., 2005). Yet, despite this important role of the amygdala in discriminating between sensory cues with opposing valence, which can in turn drive behavior in different directions (i.e., approach vs. avoidance), it remains to be determined whether and how its functional connectivity patterns with other brain regions vary during different types of motivated behaviors and their modulation by different goal states.

In our study, to vary the affective value of experimental events and elicit different actions in response to them, we manipulated appraisals of goal conduciveness and coping potential during an arcade game where participants navigated a maze with the aim of making as many points as possible. These two appraisals produce strong effects on subjective emotional experience and motivated behavior (Sander, Grandjean, & Scherer, 2005). In particular, goal conduciveness appraisals (also called goal (in)congruence or motivational valence; Lazarus, 1991; Frijda, 1986) evaluates the effect an event has on one's current goal (maximizing the game score in our context) by comparing the encountered situation with an internal representation. As a manipulation of goal conduciveness, participants could encounter good, bad, or neutral "monsters" (that respectively gave points, removed points, or had not effect). Thus, both good and bad monsters were goal relevant, but they had opposite emotional valence. As such, good and bad monsters were expected to affect the direction of motivated behaviors, with good monsters inducing more approach and bad monsters more avoidance strategies, albeit with variable degrees across trials and participants. Orthogonally to this, coping potential was manipulated by providing (or not) participants with a "superpower potion" that, once activated by the participants through a dedicated button press, altered the points gained or lost through good and bad monsters, respectively. As such, activating the superpower allowed participants to adapt to the good/bad consequences of the monsters by altering them to their advantage. This manipulation was expected to modulate, but not change, the direction of goal-directed behaviors, as the overall valence of the good and bad monster conditions remained unaltered. The validation of this manipulation was confirmed in a previous study (Leitão et al., 2020) where behavioral ratings (i.e., dominance and coping potential) were found to be higher for the power compared to the no-power conditions. By manipulating appraisal conditions, we were able to measure for quantitative changes in motivated actions in relation to current goals rather than just based on dichotomous valence categories.

To identify approach and avoidance action tendencies, we extracted different indices from participants' gameplay that provided quantitative proxies characterizing these two types of behaviors. By comparing conditions associated with approach and avoidance behaviors, respectively, we could uncover how the amygdala dynamically interacts with other brain regions during these two opposite motivational contexts. Importantly, we used multivariate analyses (partial least squares correlation [PLSC]) to relate amygdala connectivity with motivation indices computed from individual game performance. This allowed us to identify, in a data-driven way, distinct and coordinated behavioral patterns that were not immediately apparent from the averaged motivation indices themselves (e.g., reflecting efficient vs. inefficient approach or avoidance, active/strategic vs. passive/reactive avoidance) and then link those to changes in amygdala functional connectivity patterns. In doing so, we aimed to achieve a richer characterization of dynamic amygdala interactions with other brain systems during approach and avoidance behaviors.

METHODS

Participants

Twenty-six right-handed participants with no history of neurological or psychological illness were included in the analyses (14 men; mean age: 23.81 years; *SD*: 4.71 years). The mean laterality quotient score on the Edinburgh Handedness inventory (Oldfield, 1971) was mean = 74, *SD* = 19.1 (with values ranging from −100 [completely left-handed] to 100 [completely right-handed]). Mean depression scores on the Beck Depression Inventory (Beck & Steer, 1984; Beck, Erbaugh, Ward, Mock, & Mendelsohn, 1961) equaled mean = 4.96, *SD* = 5.64 (depression scores taking values from 0 to 63, all scores < 30, the recommended threshold value for participation in the study). Three additional participants were excluded from analyses, respectively, because of left-handedness, drowsiness during scanning, and excessive movement. Participants had normal or corrected-to-normal vision. All gave written informed consent, and the study was approved by the research ethics committee of the canton of Geneva.

Amygdala Localizer

Experimental Design

Functional connectivity between the amygdala and the rest of the brain was evaluated with psychophysiological interaction analyses using an amygdala ROI as a seed (see below). The functional amygdala localizer was based on a paradigm first introduced by Hariri et al. (Hariri, Bookheimer, & Mazziotta, 2000), extensively used and modified to study amygdala function and emotion (Zhou

et al., 2008; Manuck, Brown, Forbes, & Hariri, 2007; Fisher et al., 2006; Hariri, Tessitore, Mattay, Fera, & Weinberger, 2002), providing robust and replicable fMRI responses. Briefly, our localizer consisted of four blocks of a perceptual emotion-matching task that alternated with four blocks of a sensorimotor control task (counterbalanced order across participants). During emotion-matching blocks, participants viewed three faces presented in an upright triangular disposition and were instructed to select the bottom face whose emotion expression matched that of the upper target face. Faces displayed fearful and angry expression pictures (black and white frontal views from the Karolinska Directed Emotional Faces database; Lundqvist, Flykt, & Öhman, 1998), balanced for emotion category and gender within each block (ID codes of pictures used: AF16, AF26, AF29, BF13, BF22, BF28, AM01, AM05, AM08, AM11, AM23, AM35). During control blocks, participants viewed three geometrical shapes presented in the same triangular disposition and were instructed to select the bottom shape that exactly matched the upper target shape. There were six distinct geometrical shapes in total, consisting of one circle and ellipses oriented either horizontally, vertically, or diagonally toward the left or right. A variable ISI of 1–2 sec was introduced before each stimuli, and all blocks were preceded by a brief instruction ("Match Emotion" or "Match Shapes") lasting 2 sec. Each block consisted of six trials presented for 5 sec each, resulting in total block length of 30 sec and a total task time of approximately 268 sec.

Behavioral Data Analyses

For completeness, we calculated the accuracy (% correct responses) and RTs for each condition in the localizer. Mean accuracy for emotion-matching trials was 91.3% (SD = 0.08%), lower than for control trials (mean = 96.2%, SD = 0.04%; one-sided Wilcoxon signed-ranks test: $z = -2.49$, $p = .006$, $d_{av} = .8$). Mean median RTs on correct trials was 1.742 msec (SD = 397 msec) for emotion-matching trials, significantly longer than for control trials (mean = 874 msec, SD = 233 msec; one-sided Wilcoxon signed-ranks test: $z = 4.36$, $p < .001$, $d_{av} = 2.75$). These differences accord with previous reports using this task (Hariri et al., 2000).

fMRI Data Analyses

Because of technical issues, the amygdala localizer data of one participant was not acquired, which resulted in a total of 25 participants for the functional identification of the amygdala. The localizer data were analyzed with SPM12 (Wellcome Department of Imaging Neuroscience; www.fil.ion.ucl.ac.uk/spm; Friston et al., 1994) and modeled at the subject level as a block design with two experimental conditions (EMO and SHAPE). We also included an instruction block regressor and an event-related regressor for response keypresses, shared across the two stimulus conditions. All regressors were convolved with the canonical hemodynamic response function. In addition, given behavioral differences in RTs, we also included an additional parametric regressor modeling trial-specific RTs in each condition, ensuring we could compare stimulus-related activations between the two conditions, rather than task difficulty differences (Taylor, Rastle, & Davis, 2014). Nuisance covariates included realignment parameters to account for residual motion artifacts. For each participant, condition-specific effects were then estimated using the general linear model (GLM) to compute contrast images for each condition. Finally, at the second level, we identified functionally responsive voxels in the amygdala by contrasting the EMO > SHAPE conditions using a random effect paired t-test analysis (Friston, Holmes, Price, Buchel, & Worsley, 1999). Voxels were selected based on a height threshold of $p < .05$ corrected for multiple comparisons (FWE rate) within the entire brain.

Amygdala Seed

A bilateral amygdala mask was created from the localizer data and used as a seed region in further analyses. To guarantee that all functional seed voxels were strictly located in the amygdala, this mask was further restricted to voxels overlapping with an anatomical mask derived from the CIT168 atlas (Tyszka & Pauli, 2016). Specifically, we binarized the "CIT168_iAmyNuc_1mm_MNI" image, dilated it using the *spm_dilate* function to guarantee contiguity between different subnuclei, and resliced it to the voxel size of our functional images. Finally, we selected voxels lying in the intersection between the two masks (Figure 1).

Given that this anatomical atlas contains information about different amygdala subnuclei, for completeness, we also characterized our functional amygdala mask by calculating its overlap (in terms of number of voxels) with each of these subnuclei (Table 1). Note, however, that the spatial resolution of our fMRI paradigm did not intend to make specific inferences concerning different amygdala nuclei.

Game Task: Manipulating Value in a Behaviorally Relevant Environment

Experimental Design

We used the same task as reported in our previous study (Leitão et al., 2020). Participants played a video game as a yellow agent who navigated different mazes (Figure 2) across different levels (or trials), with the goal of collecting as many points as possible and then reaching a final target location. Points could be obtained by picking coins up along the avatar's way (5 points each). At the beginning of each trial, 12 coins were displayed and distributed throughout the maze. When all these coins were picked

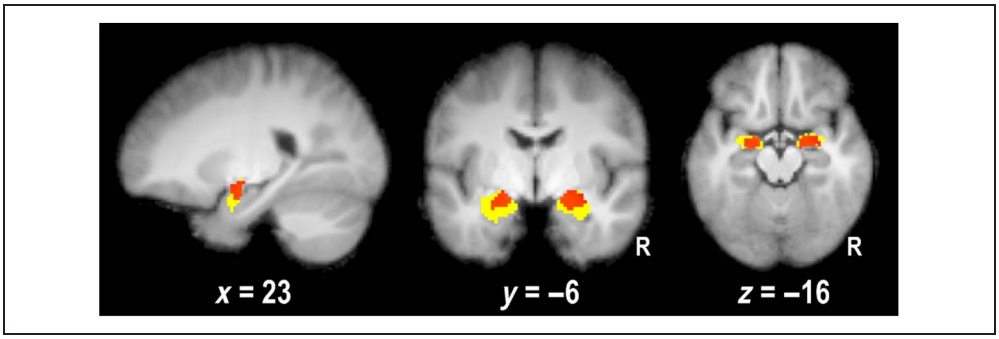

Figure 1. Visualization of the amygdala mask used in gPPI analyses. The functional amygdala ROI (red) and the anatomical amygdala mask (yellow) are shown on sagittal, coronal, and axial slices of a mean brain image created by averaging the participants' normalized structural images.

up, additional coins would appear one by one at random times and random places.

This design allowed us to manipulate two different appraisal conditions across different levels. First, we varied goal conduciveness by introducing, on each level, one monster that also navigated in the maze and could exhibit one of three possible behaviors (in different trials). These behaviors were signaled by the monster's color and shape. The neutral monster moved randomly, and touching it had no consequences for the participant. The good monster chased the player with .85 probability and moved randomly otherwise. Touching it yielded 10 points. Good and neutral monsters moved with the same speed as the player. In contrast, the bad monsters moved faster and continuously chased the player. Touching it made the participant lose 100 points. Hence, the manipulation of goal conduciveness implied differences in valence, which motivated different types of goal-directed behaviors (see Behavioral Data Analyses below).

Second, we varied coping potential by giving, on half the trials, the possibility for participants to activate a superpower. The superpower option was signaled by a small "magic potion" icon blinking on top of the yellow avatar. When activating power (by pressing a dedicated key at any time during the trial), the avatar changed its color from yellow to orange, and touching monsters led to different outcomes. Good monsters now yielded 100 points, whereas bad monsters mitigated the loss to 10 points. Consequences of touching neutral monsters remained unaltered (baseline condition). Once activated, the superpower was present until the end of the trial. The coping potential option thus allowed participants to actively change the value of good and bad monsters.

Together, this resulted in a 3 × 2 design with factors of (i) goal conduciveness (good, neutral, bad monsters) and (ii) coping potential (no-power, power; Figure 2). These two factors were manipulated across game levels, according to a standard block design (each navigation period in the maze corresponded to one block).

To proceed to the next trial/level, participants had to move their avatar to a teleporter at the top of the maze (Figure 2). This teleporter was placed behind a closed door that opened automatically after a certain time. To avoid having participants navigating in the maze indefinitely, a countdown (CD) period was introduced that set a time delay (4 sec for neutral, 6 sec for good and bad monsters) during which participants had to reach the teleporter once the door was opened. If they did not reach the teleporter within the allotted time, all points gathered during that level were lost. The CD was signaled by an audiovisual cue. Each pre-CD block lasted 8 sec, ensuring the same amount of time for each experimental condition, whereas the CD itself varied but was modeled separately. Reaching the teleporter was followed by a brief interval (1.5 sec) before the next level.

Participants played three runs inside the MRI scanner, each comprising 72 levels and lasting approximately 15 min. This amounted to 12 blocks per condition per

Table 1. Anatomical Characterization of the Functional Amygdala Seed

	Anatomical Amygdala Subnuclei									
	Deep Group or Basolateral Complex				*Superficial Group*		*Remaining Nuclei*			
		BLN								
	La	*BLD + BLI*	*BLV*	*BM*	*CMN*	*ATA*	*ASTA*	*CEN*	*AAA*	*Other*
#Voxels Overlap	5	25	6	31	67	5	14	10	12	28

AAA = anterior amygdala area; ASTA = amygdalostriatal transition; ATA = amygdala transition areas; BLN = basolateral nucleus; BLD + BLI = dorsal and intermediate subdivisions; BLV = ventral subdivision; BM = basomedial nucleus; CMN = cortical and medial nuclei; CEN = central nucleus; La = lateral nucleus; Other = amygdala voxels that are not assigned to any particular nucleus (see also Tyszka, J. M., Pauli, W. M. In vivo delineation of subdivisions of the human amygdaloid complex in a high-resolution group template. Hum Brain Mapp. 2016;37(11):3979–98, for nomenclature and grouping criteria).

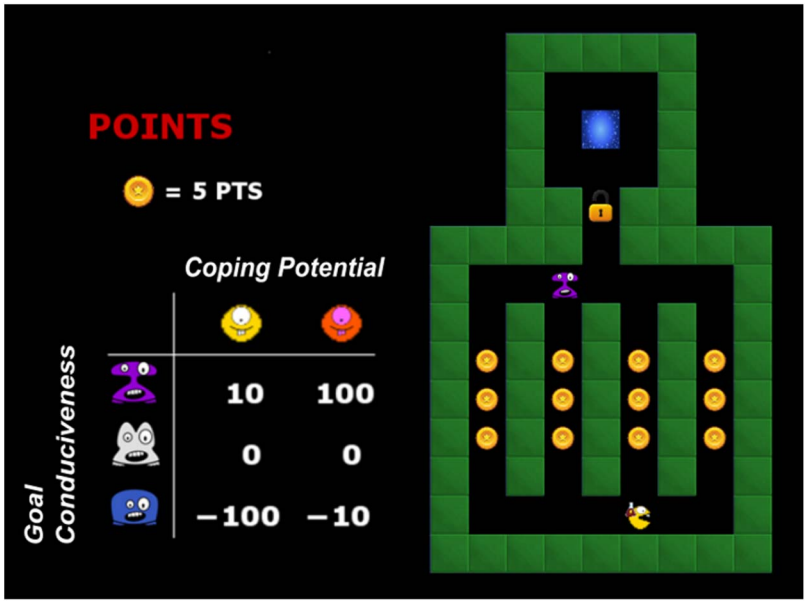

Figure 2. Illustration of the interactive video game. Example of the maze interface in one trial. The maze configuration and colors varied across trials within each condition. Experimental conditions were defined by a 3 × 2 design manipulating appraisals of (i) goal conduciveness (good, neutral, bad monsters) and (ii) coping potential (no-power, power). The colors and shapes of bad and good monsters were counterbalanced across participants.

run, and 36 blocks per condition in total. The order of conditions was pseudorandomized such that all possible transitions between different conditions took place approximately the same number of times.

The level score and the overall run score were presented to the participants at one side of the maze throughout the entire gameplay, thereby providing continuous feedback on their performance. In addition, during the second and third runs, the best score obtained in the previous runs was displayed and participants were encouraged to try beating their previous score. This display aimed at maintaining/increasing the motivation to obtain a good score across the different runs and thereby promote continuous task engagement and efficient approach and avoidance behaviors. Participants were also told that they would receive a bonus compensation proportional to their best score (though all received the same maximum bonus in the end).

To ensure that participants were able to navigate properly in the game and appraise the monster behaviors reliably, and to minimize learning effects during fMRI, we first gave a training session outside the scanner. This training session took place on the same week as the fMRI session, with an average interval of 4.28 ± 0.84 (± *SD*) days. For more details on training, please refer to our previous report (Leitão et al., 2020). Moreover, to ensure clear game conditions, a table reminding the consequences of each monster in each power levels (see Figure 2) was displayed throughout the entire gameplay, such that participants did not have to learn or rehearse the different monster properties actively in working memory during the game itself. Finally, to move the avatar in the maze, participants only needed to press a key when wanting to change direction or after they were stopped by encountering a monster, which minimized the number of necessary keypresses. For information on the visual and auditory stimuli used, please refer to the work of Leitão et al. (2020). Briefly, the color and shape of good and bad monsters, as well as the auditory sound triggered by touching them, were counterbalanced across participants.

Behavioral Data Analyses

Our goal conduciveness manipulation introduced two goal-relevant conditions with opposite emotional valence, namely, the good and bad monsters. To confirm that good and bad monster conditions (across coping potential levels) were indeed differentially evaluated as being of positive and negative valence, respectively, at the end of the scanning session, we asked participants to judge different game conditions in terms of valence (using four repetitions per condition) based on screenshots simulating events encountered during the game. These screenshots depicted the player and monster avatars placed randomly within the maze but always at a specific distance from each other, which was calculated in a participant-specific manner based on the average distance between the two characters during actual gameplay. Apart from monster type and player superpower state representing the current condition, no further information (score, coins, etc.) was displayed in these screenshots.

Ratings were performed using a bipolar 5-point Manikin scale (Leitão et al., 2020), which was converted into a scale ranging from one to five (1 representing the *negative* and 5 the *positive* edge of the scale). Individual ratings were averaged across the four repetitions and coping potential levels separately for good (mean = 4.43, *SD* = 0.61) and bad (mean = 2.49, *SD* = 0.83) monster conditions and entered into a second-level one-sided Wilcoxon signed-ranks test, indicating that ratings for the good monsters

were significantly higher than the ratings for the bad monster conditions ($z = 4.37, p < .001, d_{av} = 2.69$).

Thus, based on their valence, good compared to bad monster conditions should elicit different action tendencies, with good monsters provoking approach and bad monsters prompting avoidance behaviors. To derive measures of approach and avoidance motivation across experimental conditions, we calculated different action tendencies indices from participants' gameplay. For each condition, we calculated (i) the average number of times the player was caught from the back ("tail"; avatar facing away from the monster when touched, representing [failed] avoidance) or (ii) caught from the front ("head"; avatar facing toward the monster when touched, representing [successful] approach); (iii) the duration of CDs (the longer, the higher the potential to win or lose extra points with good or bad monsters, respectively); and (iv) the number of coins collected in a level ("coins"; indicating a change from focusing on the monster to focusing on the coins in order to gain points).

Thus, bearing in mind the game goals, an active and more efficient goal-directed *approach* behavior during good monster conditions should be characterized by a high count of the "head" and "CD" indices to maximize the number of points gained. In addition, active "head" approaches should be prioritized over more passive "tail" approaches, and monsters should be prioritized relative to coins as a source of points. In contrast, during bad monster conditions, an efficient goal-directed *avoidance* behavior should be characterized by a low count of both "head" and "tail" indices, as well as of the "CD" index, so as to minimize the number of points lost. "Tail" over "head" caught events should prevail. In addition, a high count of the "coin" index would compensate the potential loss of points caused by the bad monster and hence also correspond to more efficient outcomes. Hence, on average, we expected to see an increase in the "head" and "CD" indices for good relative to bad monster conditions, but an increase in the "tail" index for bad relative to good monsters conditions, representing approach and avoidance tendencies, respectively. Neutral monster conditions were introduced as a baseline condition where participants were expected to focus solely on coins, without specific action tendencies toward the monsters, as these do not have any effect (corresponding to low count on the "head" and "tail" indices for this condition; Table 2). Because of this, the neutral monster conditions will not be considered to evaluate approach and avoidance behaviors.

On the other hand, the coping potential manipulation was hypothesized to induce different degrees of approach and avoidance within both the good and bad goal conduciveness levels (e.g., more frequent approach of good monster in power vs. no-power conditions), but with no effect on the direction of behavior per se (i.e., no-power vs. power conditions should not induce a reversal from approach to avoidance or vice versa), a hypothesis that was confirmed behaviorally in previous work (Leitão et al., 2020). In addition, unlike goal conduciveness, the coping potential manipulation was not associated with amygdala connectivity changes (see Results below). Hence, we will focus on behavioral indices pooled (i.e., averaged) over coping potential levels (Table 2). Mean values of action tendencies indices across different conditions are provided in our previous report (Leitão et al., 2020).

To compare approach versus avoidance behaviors across good and bad monster conditions, we performed a 2 (Goal Conduciveness: good, bad) × 2 (Encounter Type: "head," "tail") repeated-measures ANOVA focusing on the indices linked to action tendencies toward the monsters (a q-q plot confirmed that the residuals were normally distributed), followed by post hoc two-sided Wilcoxon signed-ranks tests on the simple main effects. In addition, for the "CD" and "coin" indices, we performed two-sided paired *t* tests to compare good and bad monsters conditions. In total, this yielded six pairwise comparisons and we report results corrected for multiple comparisons using Bonferroni correction.

We also report two supplementary indices, namely, the number of points gained on each level type and the keypress rate made until the CD period, averaged across coping potential for each goal conduciveness level, as these indices are indicative of the individual level of goal

Table 2. Behavioral Measures Averaged across Participants (± Standard Deviation)

	Behavioral Indices	*Good*	*Neutral*	*Bad*
Action Tendencies	# tail	.44 ± .27	.04 ± .02	1.59 ± .34
	# head	4.11 ± 1.08	0.61 ± .12	1.14 ± .41
	CD (sec)	3.83 ± .78	2.39 ± .36	1.98 ± .38
	# coins	10.83 ± 2.00	15.60 ± .78	12.08 ± 1.06
Supplementary Variables	# points	441.39 ± 73.3	75.49 ± 4.1	17.8 ± 7.2
	keypress rate	.029 ± .006	.030 ± .004	.032 ± .003

achievement and task engagement, respectively (Table 2). These indices were used as supplementary variables in the multivariate analyses (see PLSC) to assist with the interpretation of the resulting latent component (LC).

Generalized Psychophysiological Interactions

Amygdala connectivity was analyzed using SPM12 (Wellcome Department of Imaging Neuroscience; www.fil.ion.ucl.ac.uk/spm; Friston et al., 1994) and the Generalized PPI Toolbox (McLaren, Ries, Xu, & Johnson, 2012). First, the experimental game design was modeled as a block design using a standard GLM approach. For a complete description of the SPM model parameters, please refer to our previous report (Leitão et al., 2020). Briefly, at the first level, pre-CD periods of 8 sec were modeled as the experimental blocks for each condition separately (3 Goal Conduciveness × 2 Coping Potential), and conditions were then compared by linear contrasts using the standard GLM implemented in SPM.

These data were submitted to generalized psychophysiological interaction (gPPI) analyses using the bilateral amygdala mask (see Amygdala Seed) as a seed region. Specifically, the original model was extended by introducing one regressor containing the amygdala seed time-course and six additional regressors containing the psychophysiological interaction terms (one per experimental condition). The seed time-course was defined by taking the first eigenvariate computed across all voxels within the amygdala mask. For each participant, condition-specific connectivity effects were estimated by creating contrast images for each condition-PPI regressor.

Finally, to allow for random effects analyses and inferences at the population level (Friston et al., 1999), condition-PPI contrast images were entered in a second-level repeated-measures ANOVA that modeled the two appraisal factors manipulated in our game (Goal Conduciveness and Coping Potential) and their interactions, as well as the Subject factor to account for the repeated-measures design.

At the second level, we focused on comparisons between the different levels of goal conduciveness, as this factor was hypothesized to induce stronger effects on approach and avoidance tendencies. The effects of Goal Conduciveness on amygdala connectivity were determined by comparing good and bad conditions pooled across coping potential conditions (i.e., $\text{good}_{(\text{power + no-power})}$ vs. $\text{bad}_{(\text{power + no-power})}$). For completeness, effects of Coping Potential on amygdala connectivity were also examined by comparing power and no-power conditions pooled across goal conduciveness conditions, and interaction effects between the two factors were tested with the contrasts "$\text{bad}_{(\text{no-power > power})} > \text{good}_{(\text{no-power > power})}$" and "$\text{good}_{(\text{no-power > power})} > \text{bad}_{(\text{no-power > power})}$." However, the Coping Potential and interaction effects did not show any significant difference in functional connectivity between the amygdala and other brain regions, and these data will not be considered further.

We report activation results with a voxel height threshold of $p < .001$ and clusters with $p < .05$ corrected for multiple comparisons (FWE rate).

PLSC

In order to link changes in amygdala connectivity with different motivated behaviors, we performed a PLSC analysis. PLSC is a multivariate technique that allows evaluating the shared information between two data tables that collect different measurements on the same set of observations (Abdi & Williams, 2013). Here, it allowed us to relate variations in multiple motivational indices, simultaneously computed from individual behavior during the game, to concomitant changes in functional connectivity patterns of the amygdala voxel-wise across the whole brain. When applied to neuroimaging, PLSC has the advantage of relating distributed brain patterns to either multiple behavior variables (behavior PLSC) or to different contrasts representing different experimental conditions (task PLSC; Krishnan, Williams, McIntosh, & Abdi, 2011; McIntosh & Lobaugh, 2004). This is achieved by projecting each sample of variables to a new space of (orthogonal) LCs that maximizes the covariance between the two input tables while accounting for multicollinearity within each set of variables, as successfully applied in previous studies investigating multidimensional processes (Siffredi et al., 2021; Mohammadi, Van De Ville, & Vuilleumier, 2020; Kebets et al., 2019; Zoller et al., 2019). In our case, each of the resulting LCs would thus represent a particular relationship between amygdala functional connectivity and specific patterns of motivated actions determined from behavioral indices during the gameplay.

Here, we performed a behavior PLSC analysis using the PLS toolbox available at https://miplab.epfl.ch/index.php/software/PLS. This analysis included our four behavioral motivation indices and amygdala connectivity patterns from the good and bad monster conditions, averaged across coping potential levels. Individual amygdala connectivity maps were vectorized and restricted to gray matter voxels that displayed positive beta connectivity values in the univariate PPI approach described above. We opted to restrict connectivity maps to positive values as negative connectivity betas may be hard to interpret for the purpose of our current study (but note that the use of unrestricted connectivity maps produced equivalent results). For each condition, amygdala connectivity maps were stored in a $n \times vox$ matrix X_{cond}, with n equal to the number of participants and vox equal to the number of voxels considered, and then z-scored across participants. Likewise, for each condition, z-scored behavior indices were stacked in a $n \times ind$ matrix Y_{cond}, with ind equal to the number of behavioral indices. Condition-specific matrices were stacked column-wise, resulting in a $2n \times vox$ matrix X and a $2n \times ind$ matrix Y. The association between brain

and behavior variables for each condition was then stored in correlation matrices $R_{cond} = Y_{cond}^T X_{cond}$, which were stacked column-wise to form a $2ind \times vox$ matrix R. Singular value decomposition was then applied to $R = USV^T$, resulting in a matrix S of singular values, indicating the covariance explained by each of the LCs, and two orthonormal left U and right V matrices of singular vectors (typically referred to as saliences), which represent the corresponding behavior and voxel profiles that best describe R. Latent components in the data set can thus be characterized by pairs of latent variables $L_X = XV$ and $L_Y = YU$ (the latter was actually computed condition-wise; see the work of Krishnan et al., 2011) that express the saliences relative to the observed brain and behavior measures. Typically, L_X and L_Y are referred to as brain and behavior scores, respectively, and each column pair (l_X, l_Y) forms an LC that models a relationship between brain and behavior. Thus, there are as many LCs as there are rows in the matrix R. In addition, these scores also reflect individual contributions to each LC.

As in principal component analysis (Abdi & Williams, 2010), behavior (or brain) loadings of LCs can be computed by correlating the original behavior (or brain) measures with the respective behavior (or brain) scores obtained by PLSC. Behavior loadings generally present the same profile as behavior saliences, depicting relative differences in behavioral measures and indicating how strongly each contributes to the brain–behavior correlations represented by an LC. Likewise, brain saliences express how much each brain voxel (here their connectivity with amygdala) contributes to the brain–behavior correlations described by the LC.

Significance of each of the eight (= 2*ind*) LCs obtained in our analysis was determined by permutation testing with 1000 permutations and corrected for multiple comparisons using Bonferroni correction (i.e., p values lower than .05/8 were considered significant). Stability of behavior and brain saliences was estimated using 500 bootstrap samples. Because resampling methods can cause axis rotation and alter the order of latent variables, we used Procrustes rotation to correct for this effect (Krishnan et al., 2011). Brain saliences were converted into bootstrap ratio z scores by dividing each voxel salience by its bootstrap-estimated standard deviation, and saliences with absolute ratios > 2.58 (corresponding to $p < .01$) were considered to be significantly stable through resampling. Equivalently, behavioral loadings are reported together with their 95% bootstrapped confidence intervals.

To interpret brain saliences, it is necessary to examine the relationship between the brain scores and the behavior loadings. For voxels with positive brain saliences, the portion contributing to the brain scores covaries positively with positive behavioral loadings and negatively with negative behavioral loadings. Voxels with negative brain saliences exhibit the opposite pattern. To facilitate interpretation, we also plotted each behavioral measure (i.e., our four motivation indices) against the brain scores from PLSC.

Finally, akin to what is commonly done in principal component analyses, we also considered two supplementary variables (see Behavioral Data Analyses), namely, the number of points (as a measure of behavioral efficiency) and the key press rate (as a measure of effort mobilization and task engagement). Specifically, after z-scoring these measures within each condition, we correlated them with brain and behavior scores associated with significant LCs from the PLSC analysis. Thus, supplementary variables have no influence on the LCs of the PLSC analysis and instead are used to further support our interpretations.

Linking gPPI and PLSC Connectivity Patterns

In a post hoc analysis, individual connectivity strengths between the amygdala and medial prefrontal brain regions observed in the gPPI analysis were related to individual connectivity scores resulting from our behavior PLSC analysis (see Results). For each participant, we extracted the beta values from the clusters in superior frontal cortex and OFC resulting from the gPPI analysis and averaged the beta values across voxels from each cluster. Using these values (z-scored within conditions) as additional supplementary variables in the behavior PLSC analysis allowed us to assess how individual connectivity strength between amygdala and medial prefrontal regions was related to the overall individual patterns obtained with our behavior PLSC analyses, representing the coordinated expression of amygdala-connected networks that were modulated by our motivational indices.

Stimuli Presentation

For both tasks, visual and auditory stimuli were presented using Psychophysics Toolbox Version 3.0.13 (Kleiner, Brainard, & Pelli, 2007; Brainard, 1997) running on MATLAB 2015b (The MathWorks Inc) and a 64-bit Windows 7 operating system (Microsoft).

All visual stimuli were displayed on a 23-in. LCD monitor (Cambridge Research Systems Ltd; model: BOLDscreen 23; resolution: 1920 × 1080 pixels, dimensions: 50.9 cm × 29 cm, refresh rate: 60 Hz, viewing distance: ~125 cm), seen by the participant through a mirror mounted on the MRI head coil.

Auditory stimuli were heard via HP AT01 earphones composed of an electrodynamic earphone driver and 46-cm long air tubes (Cambridge Research Systems Ltd), connected to standard-sized insert earphones (Canal Tips, Comply). The earphones were connected to the stimulus computer via an MR Confon amplifier unit (MR Confon GmbH).

Participants made responses and navigated in the game using their right hand and an MRI-compatible 5-Button Diamond Fiber Optic Response Pad (Current Designs Inc; model: HHSC-1x5-D), connected to the stimulus computer via an FIU-932-B electronic interface. During the

amygdala localizer task, participants used the yellow (left) and red (right) buttons, In the game, they used the green, pink, yellow, and red buttons to navigate up, down, left, and right, respectively, whereas the blue button was reserved to activate the superpower.

fMRI Data Acquisition

A 3-T TIM Trio System (Siemens) was used to acquire both high-resolution structural images (magnetization prepared rapid gradient echo, repetition time [TR] = 1900 msec, echo time [TE] = 2.27 msec, inversion time = 900 msec, flip angle = 9°, field of view [FOV] = 256 × 256 mm^2, image matrix 256 × 256, 192 sagittal slices, voxel size = 1-mm isotropic, 32-channel head coil) and T2*-weighted axial EPI with BOLD contrast (GE-EPI, TR = 600 msec, TE = 32 msec, flip angle = 52°, FOV = 210 × 210 mm^2, image matrix 84 × 84, 48 axial slices, slice thickness = 2.5 mm, with a multiband acceleration factor of 6, voxel size = 2.5-mm isotropic, 32-channel head coil). B_0 field maps (GR, 2D, TR = 528 msec, short TE = 5.19 msec, long TE = 7.65 msec, flip angle = 60°, FOV = 210 × 210 mm^2, image matrix 84 × 84, negative blip direction, slice thickness = 2.5-mm, 32-channel head coil) were also acquired to correct for static magnetic field inhomogeneities in the EPI images.

Functional and field map images were acquired using the same FOV, with the matrix's z direction placed axial and co-planar relative to the anterior commissure–posterior commissure line. This allowed whole-brain coverage, but only partial inclusion of the cerebellum and brainstem. Each participant took part in a total of three experimental game runs, each comprising, on average, 1490 (± 49 *SD*s) volume images, followed by one amygdala localizer run comprising, on average, 465 (± 4 *SD*) volume images.

fMRI Data Preprocessing

The fMRI data were preprocessed using SPM12 (Wellcome Department of Imaging Neuroscience; www.fil.ion.ucl.ac.uk/spm; Friston et al., 1994). Scans from each participant were realigned using the first as a reference, corrected for B_0 field inhomogeneities using phase maps obtained with the SPM12 FieldMap toolbox and co-registered to participants' anatomical images. The images were spatially normalized into Montreal Neurological Institute space using the parameters obtained from segmentation of the anatomical images, resampled to a spatial resolution of 2 × 2 × 2 mm^3 and spatially smoothed with a Gaussian kernel of 8 mm FWHM. The time-series of all voxels were high-pass filtered to 1/128 Hz and prewhitened using the *FAST* option from SPM12, which is based on exponential covariance functions and better suited for data acquired with short repetition times. The first five volumes were discarded to allow for T1-equilibration effects.

RESULTS

Characterization of Motivated Behaviors during Gameplay

To characterize motivational effects on goal pursuit in good versus bad monster conditions, we compared our indices of approach versus avoidance toward monsters during the game (Table 2).

First, we performed a 2 × 2 repeated-measures ANOVA with factors Goal Conduciveness (good, bad) and Encounter Type ("head," "tail"). This showed a significant main effect of Goal Conduciveness, $F(1, 25) = 42.85$; $p < .001$; $\eta_p^2 = .632$, a significant main effect of Encounter Type, $F(1, 25) = 167.69$; $p < .001$; $\eta_p^2 = .870$, and a significant interaction between the two factors, $F(1, 25) = 247.42$; $p < .001$; $\eta_p^2 = .908$. Post hoc one-sided Wilcoxon signed-ranks tests confirmed this interaction was characterized by both a decrease in the "tail" counts ($z = -4.46, p < .001, d_{av} = 3.85$) and an increase in the "head" count ($z = 4.46, p < .001, d_{av} = 4.08$) for bad relative to good monster conditions. In addition, there were significantly more "head" than "tail" encounters during the good monster condition ($z = 4.46$, $p < .001$, $d_{av} = 5.55$), suggestive of active directed approach. Conversely, there were fewer "head" than "tail" encounters during the bad monster condition ($z = -4.11, p < .001, d_{av} = 1.25$), suggesting that touching these monsters happened mostly when participants were escaping. These data therefore converge to indicate that good monsters elicited more frequent approach tendencies toward them, whereas bad monsters were associated with greater avoidance.

The other two motivation indices also showed significant changes between Goal Conduciveness conditions. The time spent in the CD period was longer for good relative to bad monster conditions ($z = 4.43, p < .001, d_{av} = 3.24$), and the number of coins eaten was reduced from the good to bad monster conditions ($z = -2.91$, $p = .004$, $d_{av} = .80$). The latter suggests a change in strategy from seeking points by touching monster to collecting points from coins, according to the monster type.

Altogether, these results demonstrate a consistent shift in the direction of motivated behaviors between good and bad conditions, indicating that our goal conduciveness manipulation successfully induced different approach and avoidance tendencies.

gPPIs

In order to assess global amygdala connectivity changes across game conditions, we first ran a gPPI analysis on our 3 (Goal Conduciveness: good, neutral, and bad monsters) × 2 (Coping Potential: no-power, power) experimental conditions, using the bilateral amygdala as a seed. We focused on the effects of Goal Conduciveness, as this manipulation directly manipulated the valence of monsters and strongly influenced action tendencies. Comparing good relative to bad monster conditions showed higher amygdala

connectivity with the medial OFC, right antero-superior medial frontal gyrus, left inferior frontal gyrus (IFG), as well as the posterior cingulate/retrosplenial cortex extending to lower precuneus (Figure 3, Table 3). The opposite comparison (bad > good monsters) revealed higher amygdala connectivity with the right caudate (Figure 3, Table 3). On the other hand, we found neither a main effect of Coping Potential nor any interaction between the two appraisal factors.

PLSC Analyses

To more precisely relate amygdala connectivity to behavioral patterns reflecting different motivational states expressed by different action strategies, we next performed a behavior PLSC analysis. This analysis allowed us to identify brain networks that were distinctively coupled with the amygdala according to particular profiles of action tendencies during gameplay, as estimated by our different quantitative motivation indices considered simultaneously. PLSC results revealed only one significant (p = .002) LC1 accounting for 49% of the covariance between amygdala connectivity and motivation indices. This LC displayed a significant association, $r(24)$ = .68, p < .001, between the brain and behavior scores across the two experimental conditions taken together.

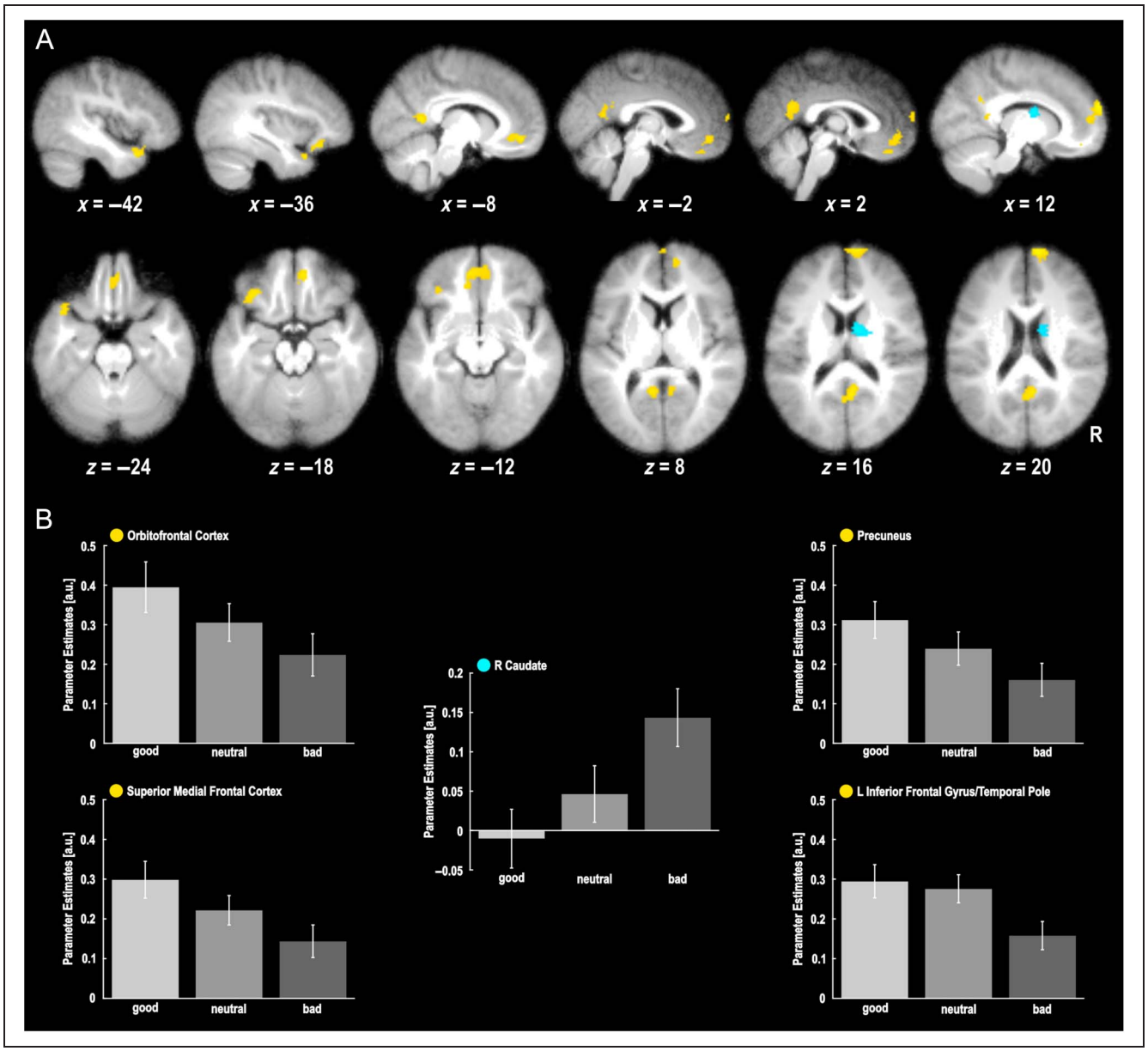

Figure 3. Differential amygdala connectivity for good versus bad monster conditions. (A) Differential increases in amygdala connectivity for good > bad (yellow) and bad > good (cyan) monster conditions. Results are presented on axial and sagittal slices of a mean brain image created by averaging the participants' normalized structural images and displayed at a voxel height threshold p < .001 with a cluster-level threshold of p_{FWE} < .05. (B) Bar plots represent mean cluster parameter estimates (± *SEM*) of connectivity for the respective brain regions, obtained by averaging voxel-wise β values from each cluster and pooling (i.e., summing) them across coping potential levels.

Table 3. Results of gPPI Analysis Using the Amygdala Seed

	MNI Coordinates (mm)					
Brain Regions	*x*	*y*	*z*	*z Score (Voxel)*	*#Voxels in Cluster*	p_{FWE}*-Value (Cluster)*
Bad > Good						
R Caudate	18	−4	12	4.16	166	.006
Good > Bad						
R Precuneus	6	−54	16	4.09	364	< .001
L Precuneus	−8	−54	10	4.08		
R Rectal Gyrus	8	44	−20	4.43	337	< .001
L Middle Orbital Gyrus	−6	46	−10	3.98		
R Superior Medial Gyrus	12	64	24	4.43	213	.001
L Superior Medial Gyrus	0	66	10	3.51		
L Temporal Pole	−40	14	−26	4.06	139	.015
L Inferior Frontal Gyrus	−34	30	−16	3.97		

MNI = Montreal Neurological Institute.

To characterize this LC1, we calculated the behavioral loadings of this component on each motivational index and each experimental condition (Figure 4B). These loadings showed that LC1 reflected a deployment of efficient strategies in goal-directed behaviors, independently of their direction, that is, regardless of whether they corresponded to approach or avoidance actions. Specifically, during good monster conditions, this LC corresponded to a strong positive expression of the "head" encounters and a negative expression of the "tail" encounters, hence reflecting *active* approach toward good monsters. Together with a more moderate but positive loading on the "CD" duration index, this behavioral pattern indicates an efficient goal-pursuit strategy to maximize gains obtained by touching the good monsters. Conversely, during bad monster conditions, there was a strong negative loading on both "tail" and "head" counts, reflecting a general avoidance of bad monsters to minimize losses. There was also a positive effect on the "coin" count, suggesting that, in addition to active avoidance, the LC was associated with attempts to collect more coins in order to compensate losses of points because of the bad monsters.

In summary, the LC identified by PLSC, linking motivated action indices to amygdala connectivity modulations, captured an overall coherent pattern of adaptive behavior to either approach or avoid monsters according to their goal relevance, but irrespective of the direction of behavior itself. Condition-wise scatterplots between brain scores and motivation indices provide a further illustration of this pattern (Figure 4C), with clear interaction effects apparent for "head" and "coin" measures.

Two other behavioral variables reinforced this interpretation. First, the number of points obtained during good or bad monster conditions was strongly positively correlated with both the brain and behavior scores for this LC, in both conditions (Table 4). This emphasizes that higher expression of this component, both behaviorally and neurally, reflects optimal adjustment of approach and avoidance according to motivational state, allowing participants to maximize their gains. Likewise, the keypress rate also showed positive correlations with brain and behavior scores, reaching significance only in the bad monster condition (Table 4), suggesting stronger motor engagement and more active effort mobilization, particularly when escaping the monsters.

At the brain level, the LC1 was associated with functional connectivity between the amygdala and an extended network of areas (positive brain saliences, Figure 4A) that comprised large regions in medial prefrontal cortices (mPFC), including ACC and medial superior frontal gyrus, as well as the bilateral IFG, bilateral insula, hippocampus, and posterior cingulate cortex. It also extended to a dorsal frontoparietal network including the superior parietal lobes and FEFs, plus several motor regions including primary motor cortices, SMAs, bilateral caudate, and cerebellum. In other words, higher functional coupling between amygdala activity and this distributed set of brain areas was associated with higher expression of *efficient* approach or avoidance behaviors, as identified by the significant LC1 from our PLSC analysis. There were only limited areas showing higher connectivity with the amygdala during *inefficient* behavior (right lateral occipital cortex, posterior insula, and cerebellar vermis; Figure 4A).

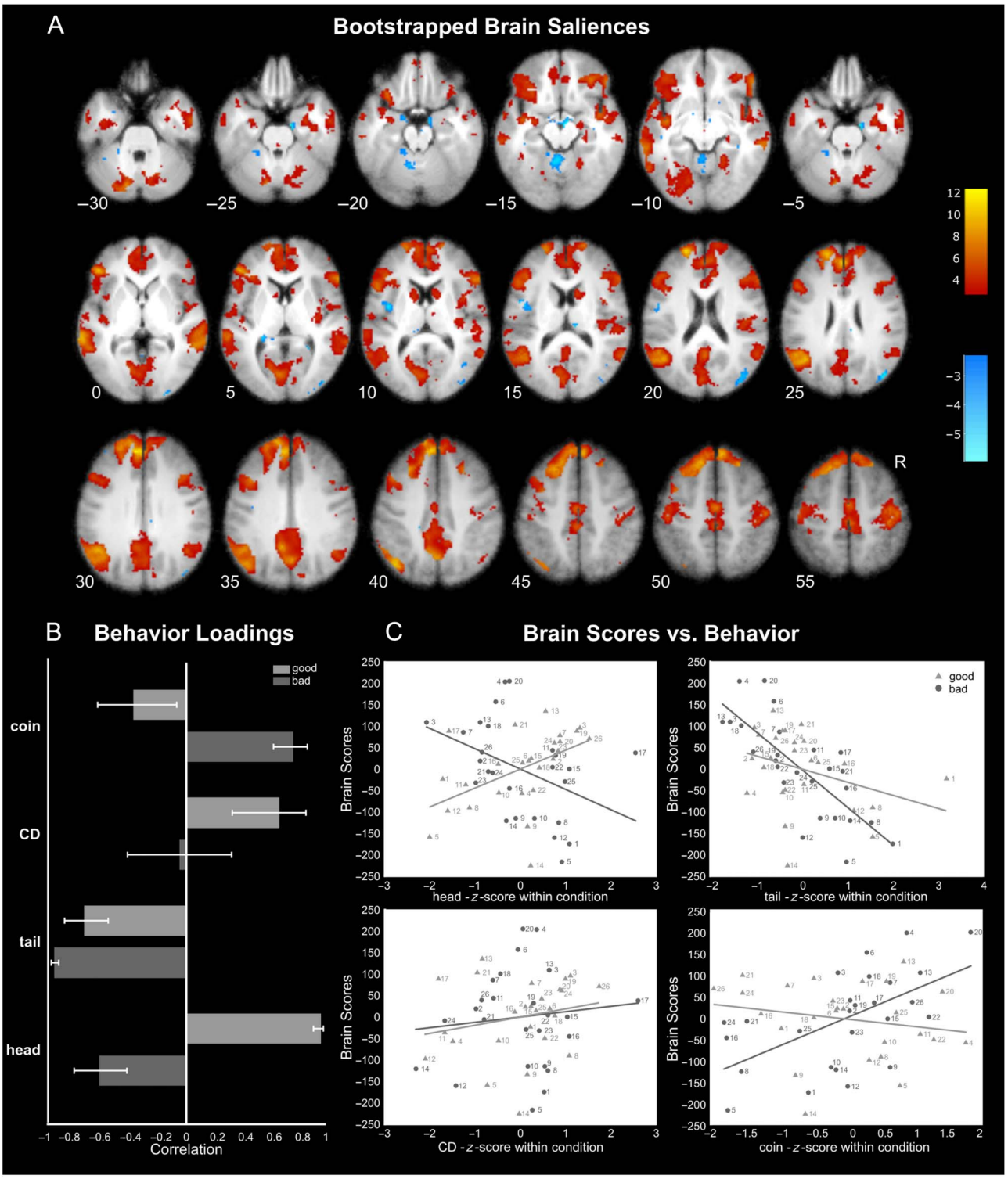

Figure 4. Latent component (LC1) from the behavior-based PLSC analysis. (A) Brain saliences of LC1 across voxels, thresholded at bootstrap ratios of ± 2.58 (corresponding to $p < .01$). Positive brain saliences are displayed in red, and negative brain saliences are displayed in blue. (B) Behavior loadings (i.e., correlation between behavioral measures and PLSC saliences) of LC1 are plotted for each of our action indices with bootstrap-estimated 95% confidence intervals for good (light gray) and bad (dark gray) monster conditions. The loading profile suggests that LC1 reflects efficient goal-directed motivation. (C) Brain scores of LC1 are plotted as a function of the magnitude of each action indices (*z*-scored), for good (light gray triangles) and bad (dark gray circles) monster conditions. The correlations indicate a reliable quantitative relationship between stronger expression of LC1 and higher occurrences of approach or avoidance toward monsters. Numbers represent individual participants.

Table 4. Pearson Correlations (p Value) between Behavior PLSC Scores (LC1) and Supplementary Variables Reflecting Goal Achievement, Task Engagement, and Amygdala Connectivity with Medial Frontal Brain Regions

		Behavior Scores		*Brain Scores*	
		Bad	*Good*	*Bad*	*Good*
Supplementary Variables	Behavioral Measures				
	# points	.94 (<.001)	.93 (<.001)	.68 (<.001)	.43 (.02)
	keypress rate	.67 (<.001)	.46 (.02)	.57 (.002)	.29 (.16)
	Amygdala Connectivity				
	Superior Medial Frontal Cortex	.44 (.02)	.33 (.09)	.63 (<.001)	.67 (<.001)
	OFC	.24 (.24)	.13 (.52)	.52 (.006)	.56 (.003)

Linking gPPI and PLSC Connectivity Patterns

Motivated behaviors are generally considered to be steered by projections from the amygdala to mpFC that can then act to recruit attentional and executive resources necessary to respond to relevant stimuli (Salzman & Fusi, 2010; Phelps & LeDoux, 2005). To examine the relationship between functional amygdala coupling with medial prefrontal brain areas (through our univariate gPPI analyses) with the more distributed connectivity pattern associated with efficient motivational effects on behavior (revealed by PLSC), we extracted individual beta values from the superior frontal cortex and OFC (from gPPI) and included them as supplementary variables in the PLSC analysis. Beta values from both clusters were positively correlated with brain scores from this new behavior PLSC analysis, in both the good and bad monster conditions (Table 4). Correlations with behavior scores were not significant. These results indicate that the stronger amygdala was functionally connected with medial prefrontal areas, the more the distributed networks associated with the LC1 component was expressed, during both approach and avoidance behaviors.

DISCUSSION

The amygdala is not only implicated in the affective appraisal of behaviorally relevant and valenced events (i.e., pleasant or unpleasant), but also ideally placed to orchestrate adaptive responses through extensive connectivity with other brain areas (Freese & Amaral, 2009; Phelps & LeDoux, 2005; Amaral & Price, 1984). Yet, the neural pathways mediating its influence on motivated action during approach or avoidance behaviors remain to be fully established, and variations in their recruitment according to the direction of motivated actions has not been systematically examined. In this study, we used fMRI to measure whole-brain functional connectivity of the amygdala and its modulation while participants were engaged in a first-person interactive game where they had to make goal-directed responses with opposing motivational directions. Critically, two different appraisals were manipulated: goal conduciveness (with different monster types) and coping potential (with different power states). As expected, goal conduciveness effectively modulated subjective valence experienced with good or bad monsters (see Methods: Behavioral Analyses), and thus steered participants into opposite motivated behaviors. Critically, our paradigm enabled us to compute several behavioral indices derived from each individual's gameplay to quantitatively measure approach and avoidance, which neatly converged to show that participants reacted to monsters by moving toward the good ones (as reflected by increases in "head" and "CD" counts) but away from the bad ones (as reflected by decreases in "head" and "CD" counts and increases in "tail" counts). This difference in approach and avoidance behaviors was paralleled by differential amygdala connectivity patterns, with higher functional coupling to distributed regions encompassing the OFC, mPFC, IFG, and posterior cingulate during good relative to bad monster conditions, but conversely higher functional coupling to the right caudate during bad relative to good monster conditions.

On top of its role in motor functions, the caudate also contributes to affective and cognitive behaviors (Haber, 2016; Grahn, Parkinson, & Owen, 2008). Although initially held that direct amygdalostriatal pathways were restricted to the nucleus accumbens and ventral striatum, there is now clear neuroanatomical evidence for more extensive connectivity, including with the dorsal caudate (Zorrilla & Koob, 2013), as found here (Figure 3). It is thought that the amygdala might modulate activity in the striatum according to current motivational states, thereby facilitating the translation of value into action (Zorrilla & Koob, 2013). Interestingly, there is an overlap in the topographical organization of prefrontal-striatal and amygdalostriatal projections, forming a triangular arrangement of amygdalo-cortical-striatal circuits (Zorrilla & Koob, 2013). Thus, the amygdala might recruit corticostriatal circuits to strengthen the representation of action-outcome

contingencies and goal-directed action plans encoded in the caudate through inputs from pFCs. However, a cautionary note is that gPPIs cannot determine directionality or causality between functionally connected regions, and although this interpretation is compatible with our results, it would need to be confirmed with other suitable methods in future studies.

In any case, a predominance of this connectivity pattern in the bad monster condition might accord with differences in strategic planning during avoidance. The movements of bad monsters were directly targeted toward the participant's avatar, which induced more reactive and urgent avoidance of bad monsters, as opposed to more controlled and progressive approach of good monsters. These more rapid and timely skilled motor responses to bad monsters might have engaged more subcortical striatal circuits (i.e., when being chased), relative to anticipatory action control associated with good monsters (i.e., when chasing them). This interpretation also accords with a previous study where active avoidance was investigated in the context of a threat imminence continuum with high or low probability of being caught by a "predator" that resulted in the delivery of an electric shock (Mobbs et al., 2009). In the latter study, postencounter defensive reactions were defined by the anticipation of potential threat and active escape in response to imminent threat. Active escape produced subcortical activations in right striatum and midbrain, whereas threat anticipation itself activated the ventral mPFC, hippocampus, and amygdala. However, these cortical activations partially overlap with amygdala connectivity patterns found in this study for the comparison of good relative to bad monster conditions. Although good monsters did not cause an anticipation of threat, they implied an anticipatory component in terms of action planning to catch the good monsters, suggesting a more general role in motivated action rather than specific avoidance tendencies. Future studies should further design more balanced manipulations to induce different gradients of approach and avoidance, while controlling for differences in strategic planning and particular reactive behaviors. On the other hand, increased connectivity between amygdala and prefrontal areas in OFC, mPFC, and IFG for the good monster condition may reflect the difference in valence between conditions driving motivated actions in the appropriate direction. Both OFC and mPFC are consistently recruited during tasks requiring affective value comparisons (Rolls & Grabenhorst, 2008). Here, parameter estimates from these medial brain regions showed a linear decrease across the three goal conduciveness levels from good to bad (Figure 3), consistent with a graded valence representation (Anderson et al., 2003), whereas the IFG exhibited a more abrupt pattern distinguishing the bad monster condition from the other two conditions. Speculatively, one interpretation could be that although the behavioral relevance of different situations is detected by the amygdala (Sander et al., 2003), their relative value is represented through its interaction with medial prefrontal regions (Tye, 2018). This value signal might be transmitted to the IFG, which would then mediate the selection of approach (good monster and coins) or avoidance (bad monsters) behaviors. In keeping with this, previous neuroimaging and neuropsychology work suggests that IFG plays an important role in action selection mechanisms and their modulation by emotion (Sagaspe, Schwartz, & Vuilleumier, 2011), with left IFG implicated in resolving competition between different motor responses and right IFG preferentially recruited by inhibition of prepotent responses (Aron, Robbins, & Poldrack, 2014; Rey et al., 2014).

Moreover, the medial brain regions activated for good relative to bad monster conditions partly overlap with those reported in another previous study that used an active avoidance task performed under two different threat contexts (Gold, Morey, & McCarthy, 2015). Similar to ours, their study manipulated the presence/absence of an unpredictable threat (electric shocks delivered at random times), while participants performed a dual task of avoiding a predator (akin to our bad monsters) and catching prey (akin to our coins). Their results showed increased functional connectivity of the amygdala with mpFC as well as with precuneus and extensive areas in the lateral pFCs, for threat relative to nonthreat conditions. Given that performance measures (number of preys caught and number of times caught by predators) were kept constant across threat manipulations, the authors concluded that these cortical–subcortical interactions helped protect goal pursuit in the face of threat and mediated the regulation of anxiety. However, the direction of their findings may seem at odds with ours. Indeed, although we did not manipulate threat orthogonally to task demands as Gold et al. did (precluding direct comparison), we found higher prefrontal–amygdala connectivity in the good (relative to the bad) monster condition, which was less threatening and previously found to induce lower anxiety ratings (Leitão et al., 2020). On the other hand, a commonality between their unpredictable threat condition and our good monster condition is the fact that both included an element of uncertainty. In fact, whereas the bad monsters chased participants at all times, the good monsters followed participants with a probability of .85 and moved at random otherwise, presumably requiring participants to consider this ambiguity when planning their behavior. In addition, in the good conditions, both touching the monster and collecting coins yielded points, which added ambiguity regarding the most appropriate behavior in that condition. Other observations support a role of the amygdala in responding to ambiguous or uncertain situations that are behaviorally relevant (Rosen & Donley, 2006; Whalen, 1998) or to unpredictability of sensory events (Herry et al., 2007). Likewise, mpFC regions may activate to the anticipation of stimuli with ambiguous valence and have been shown to be involved in the processing of decisional uncertainty (Levy, Snell, Nelson, Rustichini, & Glimcher, 2010; Critchley, Mathias, & Dolan,

2001; Bechara, Damasio, & Damasio, 2000). Therefore, increased connectivity observed between the amygdala and medial brain areas might instead signal decisional ambiguity, summoning participants to process additional information and prepare to flexibly adapt to contingencies in order to maintain an efficient goal-pursuit (Pessoa, 2010; Whalen, 1998). In fact, in our study, individual connectivity strengths between the amygdala and mpFC areas were positively correlated with brain scores from a significant PLSC LC representing efficient approach and avoidance behaviors (Figure 4), that is, irrespective of motivational direction (Table 4). These associations tentatively suggest that amygdala interactions with medial prefrontal regions captured the overall subjective salience of ongoing events that drove the motivation and efficacy of motor actions, regardless of the valence and direction of actual responses (e.g., approaching or avoiding the monster, collecting more points or rushing during the CD; Janak & Tye, 2015; Sander et al., 2003).

In fact, unlike the univariate gPPI comparing conditions in a block-wise manner, the multivariate PLSC approach allowed linking amygdala connectivity patterns with several motivation measures that simultaneously co-varied during game performance. Specifically, this analysis allowed us to extract, in a data-driven way, behavioral patterns that were not immediately observable from the motivation indices alone. This approach revealed only one dominant LC that reflected the efficiency of avoidance or approach tendencies when confronted with different (goal-conducive or obstructive) monster conditions (Figure 4B, Table 4), and involved an extensive network of dorsal frontoparietal areas and motor regions at the brain level (Figure 4A). These areas are associated with motor control and attentional processing, which further highlights that amygdala activity directly promoted actions necessary to adapt to environment contingencies. In fact, unlike more reflexive affective behaviors such as freezing, approach to a reward and avoidance of an aversive stimulus both require a coordinated engagement of attentional, executive, and motor circuits involved in action planning and execution to allow successful goal-pursuit. This connectivity pattern is consistent with influences from the amygdala on attentional resources (Pourtois, Schettino, & Vuilleumier, 2013; Vuilleumier, 2009), integrating information about stimulus value and relevant spatial locations (Peck & Salzman, 2014; Peck, Lau, & Salzman, 2013), and promoting swift motor action to them (Grezes, Valabregue, Gholipour, & Chevallier, 2014; Sagaspe et al., 2011). Accordingly, brain systems associated with the PLSC LC may constitute neural pathways that directly instantiate efficient behavioral actions motivated by relevant cues, beyond the prefrontal areas identified by gPPI.

To summarize, our study suggests that through connectivity with distributed brain networks, amygdala activity is involved in driving motivational processes that are not specific to approach or avoidance actions, but instead promote the initiation and energization of behavioral responses to affectively relevant events, irrespective of motivational direction. By tracking the overall value of sensory cues, including their subjective and context-dependent significance, in coordination with prefrontal regions and executive networks, the amygdala may thus promote adaptive actions to cope with environment contingencies in affective contexts.

Acknowledgments

This study was conducted on the imaging platform at the Brain and Behavior Lab and benefited from support of the Brain and Behavior Lab technical staff.

Reprint requests should be sent to Department of Fundamental Neuroscience, Laboratory for Behavioral Neurology and Imaging of Cognition, University of Geneva, 1 rue Michel-Servet Geneva, Geneva 1211, Switzerland, or via e-mail: mjoana.leitao@unige.ch.

Author Contributions

Joana Leitão: Conceptualization; Data curation; Formal analysis; Funding acquisition; Investigation; Methodology; Software; Supervision; Visualization; Writing—Original draft; Writing—Review & editing. Maya Burckhardt: Formal analysis; Investigation. Patrik Vuilleumier: Conceptualization; Funding acquisition; Resources; Supervision; Writing—Original draft; Writing—Review & editing.

Funding Information

This study was funded by the National Center of Competence in Research [NCCR] (https://dx.doi.org/10.13039/501100002339) Affective Sciences (51NF40-104897) and a Sinergia grant from the Swiss National Science Foundation (CRII5-180319).

Diversity in Citation Practices

Retrospective analysis of the citations in every article published in this journal from 2010 to 2021 reveals a persistent pattern of gender imbalance: Although the proportions of authorship teams (categorized by estimated gender identification of first author/last author) publishing in the *Journal of Cognitive Neuroscience* (*JoCN*) during this period were M(an)/M = .407, W(oman)/M = .32, M/W = .115, and W/W = .159, the comparable proportions for the articles that these authorship teams cited were M/M = .549, W/M = .257, M/W = .109, and W/W = .085 (Postle and Fulvio, *JoCN*, 34:1, pp. 1–3). Consequently, *JoCN* encourages all authors to consider gender balance explicitly when selecting which articles to cite and gives them the opportunity to report their article's gender citation balance.

REFERENCES

Abdi, H., & Williams, L. J. (2010). Principal component analysis. *WIREs Computational Statistics*, *2*, 433–459. https://doi.org/10.1002/wics.101

Abdi, H., & Williams, L. J. (2013). Partial least squares methods: Partial least squares correlation and partial least square

regression. *Methods in Molecular Biology*, *930*, 549–579. https://doi.org/10.1007/978-1-62703-059-5_23, PubMed: 23086857
Adolphs, R., Gosselin, F., Buchanan, T. W., Tranel, D., Schyns, P., & Damasio, A. R. (2005). A mechanism for impaired fear recognition after amygdala damage. *Nature*, *433*, 68–72. https://doi.org/10.1038/nature03086, PubMed: 15635411
Amaral, D. G., & Price, J. L. (1984). Amygdalo-cortical projections in the monkey (Macaca fascicularis). *Journal of Comparative Neurology*, *230*, 465–496. https://doi.org/10.1002/cne.902300402, PubMed: 6520247
Anderson, A. K., Christoff, K., Stappen, I., Panitz, D., Ghahremani, D. G., Glover, G., et al. (2003). Dissociated neural representations of intensity and valence in human olfaction. *Nature Neuroscience*, *6*, 196–202. https://doi.org/10.1038/nn1001, PubMed: 12536208
Aron, A. R., Robbins, T. W., & Poldrack, R. A. (2014). Inhibition and the right inferior frontal cortex: One decade on. *Trends in Cognitive Sciences*, *18*, 177–185. https://doi.org/10.1016/j.tics.2013.12.003, PubMed: 24440116
Ascheid, S., Wessa, M., & Linke, J. O. (2019). Effects of valence and arousal on implicit approach/avoidance tendencies: A fMRI study. *Neuropsychologia*, *131*, 333–341. https://doi.org/10.1016/j.neuropsychologia.2019.05.028, PubMed: 31153965
Barrett, L. F. (2017). The theory of constructed emotion: An active inference account of interoception and categorization. *Social Cognitive and Affective Neuroscience*, *12*, 1–23. https://doi.org/10.1093/scan/nsw154, PubMed: 27798257
Baxter, M. G., & Murray, E. A. (2002). The amygdala and reward. *Nature Reviews. Neuroscience*, *3*, 563–573. https://doi.org/10.1038/nrn875, PubMed: 12094212
Bechara, A., Damasio, H., & Damasio, A. R. (2000). Emotion, decision making and the orbitofrontal cortex. *Cerebral Cortex*, *10*, 295–307. https://doi.org/10.1093/cercor/10.3.295, PubMed: 10731224
Beck, A. T., Erbaugh, J., Ward, C. H., Mock, J., & Mendelsohn, M. (1961). An inventory for measuring depression. *Archives of General Psychiatry*, *4*, 561–571. https://doi.org/10.1001/archpsyc.1961.01710120031004, PubMed: 13688369
Beck, A. T., & Steer, R. A. (1984). Internal consistencies of the original and revised beck depression inventory. *Journal of Clinical Psychology*, *40*, 1365–1367. https://doi.org/10.1002/1097-4679(198411)40:6<1365::AID-JCLP2270400615>3.0.CO;2-D, PubMed: 6511949
Belova, M. A., Paton, J. J., & Salzman, C. D. (2008). Moment-to-moment tracking of state value in the amygdala. *Journal of Neuroscience*, *28*, 10023–10030. https://doi.org/10.1523/JNEUROSCI.1400-08.2008, PubMed: 18829960
Berkman, E. T., & Lieberman, M. D. (2010). Approaching the bad and avoiding the good: Lateral prefrontal cortical asymmetry distinguishes between action and valence. *Journal of Cognitive Neuroscience*, *22*, 1970–1979. https://doi.org/10.1162/jocn.2009.21317, PubMed: 19642879
Brainard, D. H. (1997). The psychophysics toolbox. *Spatial Vision*, *10*, 433–436. https://doi.org/10.1163/156856897x00357, PubMed: 9176952
Bramson, B., Folloni, D., Verhagen, L., Hartogsveld, B., Mars, R. B., Toni, I., et al. (2020). Human lateral frontal pole contributes to control over emotional approach avoidance actions. *Journal of Neuroscience*, *40*, 2925–2934. https://doi.org/10.1523/JNEUROSCI.2048-19.2020, PubMed: 32034069
Critchley, H. D., Mathias, C. J., & Dolan, R. J. (2001). Neural activity in the human brain relating to uncertainty and arousal during anticipation. *Neuron*, *29*, 537–545. https://doi.org/10.1016/s0896-6273(01)00225-2, PubMed: 11239442
Cunningham, W. A., Arbuckle, N. L., Jahn, A., Mowrer, S. M., & Abduljalil, A. M. (2011). Aspects of neuroticism and the amygdala: Chronic tuning from motivational styles (Reprinted from *Neuropsychologia*, Vol. 48, pg. 3399–3404, 2010). *Neuropsychologia*, *49*, 657–662. https://doi.org/10.1016/j.neuropsychologia.2011.02.027, PubMed: 21414464
Cunningham, W. A., & Brosch, T. (2012). Motivational salience: Amygdala tuning from traits, needs, values, and goals. *Current Directions in Psychological Science*, *21*, 54–59. https://doi.org/10.1177/0963721411430832, PubMed: 21414464
Elliot, A. J., & Fryer, J. W. (2008). The goal construct in psychology. In J. Y. Shah & W. L. Gardner (Eds.), *Handbook of motivation science* (pp. 235–250). Guilford Press.
Fisher, P. M., Meltzer, C. C., Ziolko, S. K., Price, J. C., Moses-Kolko, E. L., Berga, S. L., et al. (2006). Capacity for 5-HT1A-mediated autoregulation predicts amygdala reactivity. *Nature Neuroscience*, *9*, 1362–1363. https://doi.org/10.1038/nn1780, PubMed: 17013380
Freese, J. L., & Amaral, D. G. (2009). Neuroanatomy of the primate amygdala. In P. Whalen & E. A. Phelps (Eds.), *The human amygdala* (pp. 3–42). Guilford Press.
Frijda, N. H. (1986). *The emotions*. Cambridge University Press & Editions de la Maison des Sciences de l'Homme.
Frijda, N. H. (1987). Emotion, cognitive structure, and action tendency. *Cognition and Emotion*, *1*, 115–143. https://doi.org/10.1080/02699938708408043
Friston, K. J., Holmes, A. P., Price, C. J., Buchel, C., & Worsley, K. J. (1999). Multisubject fMRI studies and conjunction analyses. *Neuroimage*, *10*, 385–396. https://doi.org/10.1006/nimg.1999.0484, PubMed: 10493897
Friston, K. J., Holmes, A. P., Worsley, K. J., Poline, J. B., Frith, C. D., & Frackowiak, R. S. J. (1994). Statistical parametric maps in functional imaging: A general linear approach. *Human Brain Mapping*, *2*, 189–210. https://doi.org/10.1002/hbm.460020402
Gold, A. L., Morey, R. A., & McCarthy, G. (2015). Amygdala-prefrontal cortex functional connectivity during threat-induced anxiety and goal distraction. *Biological Psychiatry*, *77*, 394–403. https://doi.org/10.1016/j.biopsych.2014.03.030, PubMed: 24882566
Grahn, J. A., Parkinson, J. A., & Owen, A. M. (2008). The cognitive functions of the caudate nucleus. *Progress in Neurobiology*, *86*, 141–155. https://doi.org/10.1016/j.pneurobio.2008.09.004, PubMed: 18824075
Grezes, J., Valabregue, R., Gholipour, B., & Chevallier, C. (2014). A direct amygdala-motor pathway for emotional displays to influence action: A diffusion tensor imaging study. *Human Brain Mapping*, *35*, 5974–5983. https://doi.org/10.1002/hbm.22598, PubMed: 25053375
Haber, S. N. (2016). Corticostriatal circuitry. *Dialogues in Clinical Neuroscience*, *18*, 7–21. https://doi.org/10.31887/DCNS.2016.18.1/shaber
Hariri, A. R., Bookheimer, S. Y., & Mazziotta, J. C. (2000). Modulating emotional responses: Effects of a neocortical network on the limbic system. *NeuroReport*, *11*, 43–48. https://doi.org/10.1097/00001756-200001170-00009, PubMed: 10683827
Hariri, A. R., Tessitore, A., Mattay, V. S., Fera, F., & Weinberger, D. R. (2002). The amygdala response to emotional stimuli: A comparison of faces and scenes. *Neuroimage*, *17*, 317–323. https://doi.org/10.1006/nimg.2002.1179, PubMed: 12482086
Herry, C., Bach, D. R., Esposito, F., Di Salle, F., Perrig, W. J., Scheffler, K., et al. (2007). Processing of temporal unpredictability in human and animal amygdala. *Journal of Neuroscience*, *27*, 5958–5966. https://doi.org/10.1523/JNEUROSCI.5218-06.2007, PubMed: 17537966
Izquierdo, A., & Murray, E. A. (2007). Selective bilateral amygdala lesions in rhesus monkeys fail to disrupt object reversal learning. *Journal of Neuroscience*, *27*, 1054–1062. https://doi.org/10.1523/JNEUROSCI.3616-06.2007, PubMed: 17267559

Janak, P. H., & Tye, K. M. (2015). From circuits to behaviour in the amygdala. *Nature*, *517*, 284–292. https://doi.org/10.1038/nature14188, PubMed: 25592533

Kaldewaij, R., Koch, S. B., Volman, I., Toni, I., & Roelofs, K. (2017). On the control of social approach-avoidance behavior: Neural and endocrine mechanisms. *Current Topics in Behavioral Neurosciences*, *30*, 275–293. https://doi.org/10.1007/7854_2016_446, PubMed: 27356521

Kebets, V., Holmes, A. J., Orban, C., Tang, S., Li, J., Sun, N., et al. (2019). Somatosensory-motor dysconnectivity spans multiple transdiagnostic dimensions of psychopathology. *Biological Psychiatry*, *86*, 779–791. https://doi.org/10.1016/j.biopsych.2019.06.013, PubMed: 31515054

Kim, J., Mattek, A., Bennett, R., Solomon, K., Shin, J., & Whalen, P. (2017). Human amygdala tracks a feature-based valence signal embedded within the facial expression of surprise. *Journal of Neuroscience*, *37*, 9510–9518. https://doi.org/10.1523/JNEUROSCI.1375-17.2017, PubMed: 28874449

Kim, H., Shimojo, S., & O'Doherty, J. P. (2006). Is avoiding an aversive outcome rewarding? Neural substrates of avoidance learning in the human brain. *PLoS Biology*, *4*, 1453–1461. https://doi.org/10.1371/journal.pbio.0040233, PubMed: 16802856

Kleiner, M., Brainard, D. H., & Pelli, D. (2007). What's new in Psychtoolbox-3? *Perception*, *36*, 1–16.

Krishnan, A., Williams, L. J., McIntosh, A. R., & Abdi, H. (2011). Partial least squares (PLS) methods for neuroimaging: A tutorial and review. *Neuroimage*, *56*, 455–475. https://doi.org/10.1016/j.neuroimage.2010.07.034, PubMed: 20656037

LaBar, K. S., Gitelman, D. R., Parrish, T. B., Kim, Y. H., Nobre, A. C., & Mesulam, M. M. (2001). Hunger selectively modulates corticolimbic activation to food stimuli in humans. *Behavioral Neuroscience*, *115*, 493–500. https://doi.org/10.1037/0735-7044.115.2.493, PubMed: 11345973

Laham, S. M., Kashima, Y., Dix, J., & Wheeler, M. (2015). A meta-analysis of the facilitation of arm flexion and extension movements as a function of stimulus valence. *Cognition and Emotion*, *29*, 1069–1090. https://doi.org/10.1080/02699931.2014.968096, PubMed: 25345558

Lang, P. J., & Bradley, M. M. (2013). Appetitive and defensive motivation: Goal-directed or goal-determined? *Emotion Review*, *5*, 230–234. https://doi.org/10.1177/1754073913477511, PubMed: 24077330

Lazarus, R. S. (1991). Cognition and motivation in emotion. *American Psychologist*, *46*, 352–367. https://doi.org/10.1037/0003-066x.46.4.352

LeDoux, J. E. (2012). Evolution of human emotion: A view through fear. *Progress in Brain Research*, *195*, 431–442. https://doi.org/10.1016/B978-0-444-53860-4.00021-0, PubMed: 22230640

Leitão, J., Meuleman, B., Van De Ville, D., & Vuilleumier, P. (2020). Computational imaging during video game playing shows dynamic synchronization of cortical and subcortical networks of emotions. *PLoS Biology*, *18*, e3000900. https://doi.org/10.1371/journal.pbio.3000900, PubMed: 33180768

Levy, I., Snell, J., Nelson, A. J., Rustichini, A., & Glimcher, P. W. (2010). Neural representation of subjective value under risk and ambiguity. *Journal of Neurophysiology*, *103*, 1036–1047. https://doi.org/10.1152/jn.00853.2009, PubMed: 20032238

Lundqvist, D., Flykt, A., & Öhman, A. (1998). The Karolinska Directed Emotional Faces—KDEF. In *CD ROM from Department of Clinical Neuroscience, Psychology section, Karolinska Institutet*.

Manuck, S. B., Brown, S. M., Forbes, E. E., & Hariri, A. R. (2007). Temporal stability of individual differences in amygdala reactivity. *American Journal of Psychiatry*, *164*, 1613–1614. https://doi.org/10.1176/appi.ajp.2007.07040609, PubMed: 17898358

McIntosh, A. R., & Lobaugh, N. J. (2004). Partial least squares analysis of neuroimaging data: applications and advances. *Neuroimage*, *23(Suppl. 1)*, S250–S263. https://doi.org/10.1016/j.neuroimage.2004.07.020, PubMed: 15501095

McLaren, D. G., Ries, M. L., Xu, G., & Johnson, S. C. (2012). A generalized form of context-dependent psychophysiological interactions (gPPI): A comparison to standard approaches. *Neuroimage*, *61*, 1277–1286. https://doi.org/10.1016/j.neuroimage.2012.03.068, PubMed: 22484411

Meaux, E., & Vuilleumier, P. (2015). Emotion perception and elicitation. In A. W. Toga (Ed.), *Brain mapping: An encyclopedic reference*. Oxford, United Kingdom: Elsevier. https://doi.org/10.1016/B978-0-12-397025-1.00159-7

Mobbs, D., Marchant, J. L., Hassabis, D., Seymour, B., Tan, G., Gray, M., et al. (2009). From threat to fear: The neural organization of defensive fear systems in humans. *Journal of Neuroscience*, *29*, 12236–12243. https://doi.org/10.1523/JNEUROSCI.2378-09.2009, PubMed: 19793982

Mohammadi, G., Van De Ville, D., & Vuilleumier, P. (2020). Brain networks subserving functional core processes of emotions identified with componential modelling. *bioRxiv*. https://doi.org/10.1101/2020.06.10.145201

Moors, A. (2014). Flavors of appraisal theories of emotion. *Emotion Review*, *6*, 303–307. https://doi.org/10.1177/1754073914534477

Moors, A., Boddez, Y., & De Houwer, J. (2017). The power of goal-directed processes in the causation of emotional and other actions. *Emotion Review*, *9*, 310–318. https://doi.org/10.1177/1754073916669595

Morrison, S. E., & Salzman, C. D. (2010). Re-valuing the amygdala. *Current Opinion in Neurobiology*, *20*, 221–230. https://doi.org/10.1016/j.conb.2010.02.007, PubMed: 20299204

Murray, E. A., & Izquierdo, A. (2007). Orbitofrontal cortex and amygdala contributions to affect and action in primates. *Annals of the New York Academy of Sciences*, *1121*, 273–296. https://doi.org/10.1196/annals.1401.021, PubMed: 17846154

Oldfield, R. C. (1971). The assessment and analysis of handedness: The Edinburgh inventory. *Neuropsychologia*, *9*, 97–113. https://doi.org/10.1016/0028-3932(71)90067-4, PubMed: 5146491

Peck, C. J., Lau, B., & Salzman, C. D. (2013). The primate amygdala combines information about space and value. *Nature Neuroscience*, *16*, 340–348. https://doi.org/10.1038/nn.3328, PubMed: 23377126

Peck, C. J., & Salzman, C. D. (2014). Amygdala neural activity reflects spatial attention towards stimuli promising reward or threatening punishment. *eLife*, *3*. https://doi.org/10.7554/eLife.04478, PubMed: 25358090

Pessoa, L. (2010). Emotion and cognition and the amygdala from "what is it?" to "what's to be done?". *Neuropsychologia*, *48*, 3416–3429. https://doi.org/10.1016/j.neuropsychologia.2010.06.038, PubMed: 20619280

Phaf, R. H., Mohr, S. E., Rotteveel, M., & Wicherts, J. M. (2014). Approach, avoidance, and affect: A meta-analysis of approach–avoidance tendencies in manual reaction time tasks. *Frontiers in Psychology*, *5*, 378. https://doi.org/10.3389/fpsyg.2014.00378, PubMed: 24847292

Phelps, E. A., & LeDoux, J. E. (2005). Contributions of the amygdala to emotion processing: From animal models to human behavior. *Neuron*, *48*, 175–187. https://doi.org/10.1016/j.neuron.2005.09.025, PubMed: 16242399

Pourtois, G., Schettino, A., & Vuilleumier, P. (2013). Brain mechanisms for emotional influences on perception and attention: What is magic and what is not. *Biological Psychology*, *92*, 492–512. https://doi.org/10.1016/j.biopsycho.2012.02.007, PubMed: 22373657

Rey, G., Desseilles, M., Favre, S., Dayer, A., Piguet, C., Aubry, J. M., et al. (2014). Modulation of brain response to emotional conflict as a function of current mood in bipolar disorder: Preliminary findings from a follow-up state-based fMRI study. *Psychiatry Research*, *223*, 84–93. https://doi.org/10.1016/j.pscychresns.2014.04.016, PubMed: 24862389

Roelofs, K., Minelli, A., Mars, R. B., van Peer, J., & Toni, I. (2009). On the neural control of social emotional behavior. *Social Cognitive and Affective Neuroscience*, *4*, 50–58. https://doi.org/10.1093/scan/nsn036, PubMed: 19047074

Rolls, E. T., & Grabenhorst, F. (2008). The orbitofrontal cortex and beyond: From affect to decision-making. *Progress in Neurobiology*, *86*, 216–244. https://doi.org/10.1016/j.pneurobio.2008.09.001, PubMed: 18824074

Rosen, J. B., & Donley, M. P. (2006). Animal studies of amygdala function in fear and uncertainty: Relevance to human research. *Biological Psychology*, *73*, 49–60. https://doi.org/10.1016/j.biopsycho.2006.01.007, PubMed: 16500019

Russell, J. A. (2003). Core affect and the psychological construction of emotion. *Psychological Review*, *110*, 145–172. https://doi.org/10.1037/0033-295x.110.1.145, PubMed: 12529060

Sagaspe, P., Schwartz, S., & Vuilleumier, P. (2011). Fear and stop: A role for the amygdala in motor inhibition by emotional signals. *Neuroimage*, *55*, 1825–1835. https://doi.org/10.1016/j.neuroimage.2011.01.027, PubMed: 21272655

Salzman, C. D., & Fusi, S. (2010). Emotion, cognition, and mental state representation in amygdala and prefrontal cortex. *Annual Review of Neuroscience*, *33*, 173–202. https://doi.org/10.1146/annurev.neuro.051508.135256, PubMed: 20331363

Sander, D., Grafman, J., & Zalla, T. (2003). The human amygdala: An evolved system for relevance detection. *Reviews in the Neurosciences*, *14*, 303–316. https://doi.org/10.1515/revneuro.2003.14.4.303, PubMed: 14640318

Sander, D., Grandjean, D., & Scherer, K. R. (2005). A systems approach to appraisal mechanisms in emotion. *Neural Networks*, *18*, 317–352. https://doi.org/10.1016/j.neunet.2005.03.001, PubMed: 15936172

Scherer, K. R. (2001). Appraisal considered as a process of multi-level sequential checking. In K. R. Scherer, A. Schorr, & T. Johnstone (Eds.), *Appraisal processes in emotion: Theory, methods, research* (pp. 92–120). Oxford University Press.

Scherer, K. R. (2009). Emotions are emergent processes: they require a dynamic computational architecture. *Philosophical Transactions of the Royal Society of London, Series B: Biological Sciences*, *364*, 3459–3474. https://doi.org/10.1098/rstb.2009.0141, PubMed: 19884141

Schlund, M. W., & Cataldo, M. F. (2010). Amygdala involvement in human avoidance, escape and approach behavior. *Neuroimage*, *53*, 769–776. https://doi.org/10.1016/j.neuroimage.2010.06.058, PubMed: 20600966

Schlund, M. W., Magee, S., & Hudgins, C. D. (2011). Human avoidance and approach learning: Evidence for overlapping neural systems and experiential avoidance modulation of avoidance neurocircuitry. *Behavioural Brain Research*, *225*, 437–448. https://doi.org/10.1016/j.bbr.2011.07.054, PubMed: 21840340

Siffredi, V., Preti, M. G., Kebets, V., Obertino, S., Leventer, R. J., McIlroy, A., et al. (2021). Structural neuroplastic responses preserve functional connectivity and neurobehavioural outcomes in children born without corpus callosum. *Cerebral Cortex*, *31*, 1227–1239. https://doi.org/10.1093/cercor/bhaa289, PubMed: 33108795

Solarz, A. K. (1960). Latency of instrumental responses as a function of compatibility with the meaning of eliciting verbal signs. *Journal of Experimental Psychology*, *59*, 239–245. https://doi.org/10.1037/h0047274

Spielberg, J. M., Miller, G. A., Warren, S. L., Engels, A. S., Crocker, L. D., Banich, M. T., et al. (2012). A brain network instantiating approach and avoidance motivation. *Psychophysiology*, *49*, 1200–1214. https://doi.org/10.1111/j.1469-8986.2012.01443.x, PubMed: 22845892

Taylor, J. S., Rastle, K., & Davis, M. H. (2014). Interpreting response time effects in functional imaging studies. *Neuroimage*, *99*, 419–433. https://doi.org/10.1016/j.neuroimage.2014.05.073, PubMed: 24904992

Tye, K. M. (2018). Neural circuit motifs in valence processing. *Neuron*, *100*, 436–452. https://doi.org/10.1016/j.neuron.2018.10.001, PubMed: 30359607

Tyszka, J. M., & Pauli, W. M. (2016). In vivo delineation of subdivisions of the human amygdaloid complex in a high-resolution group template. *Human Brain Mapping*, *37*, 3979–3998. https://doi.org/10.1002/hbm.23289, PubMed: 27354150

Vuilleumier, P. (2009). The role of the human amygdala in perception and attention. In P. J. Whalen & E. A. Phelps (Eds.), *The human amygdala* (pp. 220–249). Guilford Press.

Vuilleumier, P., & Pourtois, G. (2007). Distributed and interactive brain mechanisms during emotion face perception: Evidence from functional neuroimaging. *Neuropsychologia*, *45*, 174–194. https://doi.org/10.1016/j.neuropsychologia.2006.06.003, PubMed: 16854439

Vytal, K., & Hamann, S. (2010). Neuroimaging support for discrete neural correlates of basic emotions: A voxel-based meta-analysis. *Journal of Cognitive Neuroscience*, *22*, 2864–2885. https://doi.org/10.1162/jocn.2009.21366, PubMed: 19929758

Whalen, P. J. (1998). Fear, vigilance, and ambiguity: Initial neuroimaging studies of the human amygdala. *Current Directions in Psychological Science*, *7*, 177–188. https://doi.org/10.1111/1467-8721.ep10836912

Zhou, Z. F., Zhu, G. S., Hariri, A. R., Enoch, M. A., Scott, D., Sinha, R., et al. (2008). Genetic variation in human NPY expression affects stress response and emotion. *Nature*, *452*, 997–998. https://doi.org/10.1038/nature06858, PubMed: 18385673

Zoller, D., Sandini, C., Karahanoglu, F. I., Padula, M. C., Schaer, M., Eliez, S., et al. (2019). Large-scale brain network dynamics provide a measure of psychosis and anxiety in 22q11.2 deletion syndrome. *Biological Psychiatry: Cognitive Neuroscience and Neuroimaging*, *4*, 881–892. https://doi.org/10.1016/j.bpsc.2019.04.004, PubMed: 31171499

Zorrilla, E. P., & Koob, G. F. (2013). Amygdalostriatal projections in the neurocircuitry for motivation: A neuroanatomical thread through the career of Ann Kelley. *Neuroscience and Biobehavioral Reviews*, *37*, 1932–1945. https://doi.org/10.1016/j.neubiorev.2012.11.019, PubMed: 23220696